Journal of Hydrology 593 (2021) 125846

Contents lists available at ScienceDirect

Journal of Hydrology

journal homepage: www.elsevier.com/locate/jhydrol

Research papers

# Quantifying the effects of Prairie depressional storage complexes on drainage basin connectivity

Kevin Shook *, Simon Papalexiou, John W. Pomeroy

*University of Saskatchewan, Centre for Hydrology, 121 Research Drive, Saskatoon, SK S7N 1K2, Canada*

ARTICLE INFO

This manuscript was handled by Marco Borga, Editor-in-Chief, with the assistance of Yadu Pokhrel, Associate Editor

*Keywords:*
Fill and spill runoff
Depressional storage
Wetlands
Hysteresis
Contributing area
Canadian Prairies

ABSTRACT

Runoff in many locations within the Canadian Prairies is dominated by intermittent fill-and-spill between depressions. As a result, many basins have varying fractions of their areas connected to their outlets, due to changing depressional storage. The objective of this research is to determine the causes of the relationships between water storage and the connected fraction of depression-dominated Prairie basins. It is hypothesized that the shapes of the relationship curves are influenced by both the spatial and frequency distributions of depressional storage. Three sets of numerical experiments are presented to test the hypothesis.

The first set of experiments demonstrates that where the number of depressions is small, their size and spatial distributions are important in controlling the relationship between the volume of depressional storage and the connected fraction of a basin. As the number of depressions is increased, the areal fractions of the largest depressions decrease, which reduces the importance of the spatial distribution of depressions.

The second set of experiments demonstrates that the curve enveloping the connected fraction of a basin can be derived from the frequency distribution of depression areas, and scaling relationships between the area, volume and catchment area of the depressions, when the area of the largest depression is no greater than approximately 5% of the total.

The third set of experiments demonstrates that the presence of a single large depression can strongly influence the relationship between the depressional storage and the connected fraction of a basin, depending on the relative size of the large depression, and its location within the basin. A single depression containing 30% of the total depressional area located near the outlet was shown to cause a basin to be nearly endorheic. A similar depression near the top of a basin was demonstrated not to fill and was therefore unable to contribute flows.

The implications of the findings for developing hydrological models of large Prairie drainage basins are discussed.

## 1. Introduction

The Prairie Pothole Region (PPR) of the Canadian Prairies and Northern US Great Plains (Mann, 1974) is characterized by the presence of millions of depressions, locally known as "wetlands", "sloughs" or "potholes", which store water from direct precipitation, surface runoff, and the melt of trapped windblown snow. The extent of the PPR is shown in Fig. 1. When the depressions are filled with water, they can connect and conduct water overland, and may eventually connect to a stream channel. In Canada, much of this region is designated as including "non-effective" areas for streamflow, implying that it does not contribute flow to a stream channel for events with return periods of two years or shorter (Government of Government of Canada, 2013). The spatial distribution of the non-effective region is mapped in Fig. 1. Regions designated as "non-contributing" in the USA (Baker, 2011) are not plotted because they are defined differently.

Prior research has demonstrated that the connected fractions of basins in this region which are dominated by depressional storage (i.e. the basin fractions which are connected to the outlet, and can therefore contribute flow) are variable, and depend on the state of water storage in the depressions (Shaw et al., 2012b; Stichling and Blackwell, 1957). This is a form of hydrological connectivity (Bracken and Croke, 2007) and is related to other forms of hydrological connectivity as discussed by Bracken et al. (2013). Unlike the hydrological connectivities of hillslopes, which are difficult to observe (McGuire and McDonnell, 2010), and therefore to model, the hydrological connectivities of Prairie basins

* Corresponding author.
*E-mail address:* kevin.shook@usask.ca (K. Shook).

https://doi.org/10.1016/j.jhydrol.2020.125846
Received 24 April 2020; Received in revised form 18 November 2020; Accepted 1 December 2020
Available online 30 December 2020

dominated by depressional storage can be inferred directly from the states of water in individual depressions.

Any successful hydrological model of the region must be able to simulate the behaviours of complexes of Prairie depressions, to model their effects on the fractions of basins contributing flow. The simulation of Prairie depressions is further complicated and made more necessary by the effects of artificial drainage and climate change, which are changing the responses of basins in the region (Dumanski et al., 2015).

### 1.1. Terminology

This paper follows the terminology of van der Kamp et al. (2016). The term "depression" refers to any local topographic minimum capable of holding water, whether it contains water or not. The depressions are similar to Geographically Isolated Wetlands (GIWs), which are also depressions surrounded by uplands (Tiner, 2003), although the use of the term "geographically isolated" for prairie potholes has been questioned (Mushet et al., 2015). Furthermore, Prairie depressions are not necessarily wetlands, which are defined by van der Kamp et al. (2016) to be "persistent and stable landscape features" often denoted by the presence of hydric soils.

The water within a depression is referred to as the "pond". Each pond has a maximum possible volume, area and depth, which occur when the depression is completely filled. As discussed by Leibowitz et al. (2016), when water is added to a region with depressions, the ponds may merge together. In this paper, depressions are designated by simulating their filling with water. Therefore two or more ponds which merge are considered to be as single pond filling a single depression. The maximum area and volume of water in a pond are therefore equal to the area and volume, respectively, of the depression which contains it.

The "contributing fraction" of a river or lake drainage basin is that fraction of the basin's area which is actively contributing flow to an outlet at a given instant. The "connected fraction" of a basin is the fraction of the basin for which connections exist to the outlet, whether or not water is actively flowing. Both cases require connectivity all the way to the outlet, i.e. all of the depressions on a path to the outlet must be completely filled. Because this research is concerned with the representing the states of basins, it is the connected fractions of the basin which are simulated herein. A model of the connected fraction may be incorporated within a hydrological model which by calculating runoff is then able to simulate the actively contributing fraction of a basin.

This paper also uses the terminology of Shook et al. (2015) for "runoff" which is defined as water movement as overland or shallow interflow, which may or may not reach a drainage system, rather than the more common definition as an areal depth of stream discharge. The two uses are synonymous only when all of the depressions in a basin are connected to the outlet, i.e. when the connected fraction is 1 and all runoff can reach the basin outlet.

The region which can contribute runoff directly to a given depression, without passing through any other depression, is defined as that depression's catchment. The connected area of a depression-dominated drainage basin is comprised of the areas of the connected depressions and of their catchments.

This paper frequently references the basin fractions of depressional storage, connected area, and largest pond area to normalize their values. The fractional depressional storage is the total volume of water stored in basin ponds at any time divided by the maximum possible volume of storage in the basin, which is the total volume of the depressions. The fractional connected area is the area of the basin connected to the outlet divided by the basin area. The areal fraction of the largest depression is the area of the largest depression in a basin divided by the sum of all of the depressional areas.

### 1.2. Hysteresis in Prairie basin state variables

Much of the modelling of the effects of depressional storage on

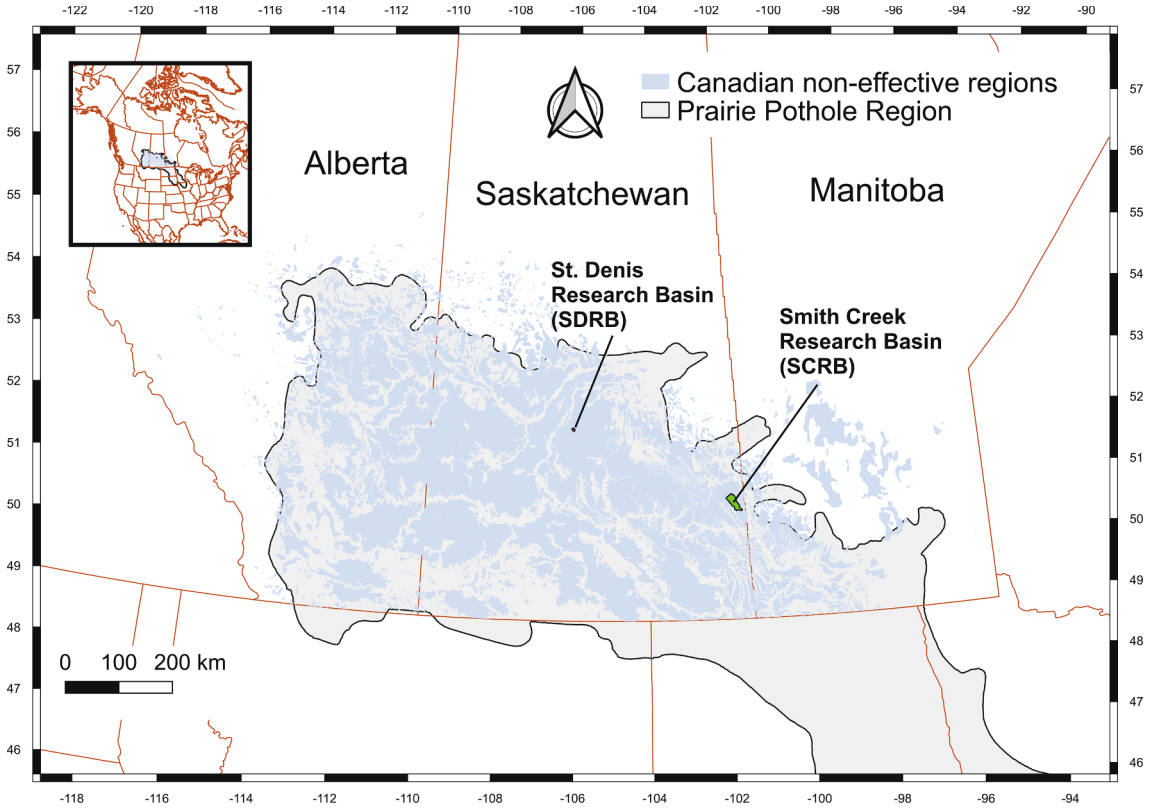


**Fig. 1.** The Prairie Pothole Region (grey shading), Canadian non-effective regions (blue shading), St. Denis Research Basin and Smith Creek Research Basin. Projection is UTM 13.

hydrology has used models which combine the storages of individual depressions into a single unit, usually by modelling them as a frequency distributions of storage (Evenson et al., 2015; Golden et al., 2014; Hossain, 2017; Mann, 1974). Although lumped methods can give good modelling results, they do not give any information about the effects of individual depressions, particularly their spatial distribution. More seriously, such methods cannot incorporate the effects of hysteresis between basin state variables.

Hysteresis has been well documented in hydrological processes at all scales (O'Kane and Flynn, 2007; Spence, 2010). The connected-area fractions of depression-dominated Prairie basins have been shown to be non-linearly and hysteretically related to water storage (Shook et al., 2015; Shook et al., 2013; Shook and Pomeroy, 2011). It has also been demonstrated that the relationship between the total volume of water stored within a basin, and its surface area is also hysteretic (Shook and Pomeroy, 2011).

The fundamental cause of the observed hysteresis in the basin-scale state variables (connected fraction and water surface area) is the existence of thousands of states, i.e. the storages of water in the depressions, within each basin. Apart from the end states, when all depressions are empty or filled, any total storage of water can be the sum of an infinite number of individual states of the water in the ponds.

The processes which affect the storage of water behave very differently in positive (additive) and negative (subtractive) directions. Additions of water may come from direct precipitation, melting of windblown snow drifts, and runoff from uplands adjacent to a depression, as well as by water transfer from other depressions through surface or shallow subsurface flows. Substantial deep groundwater inflows to or discharges from depressions are uncommon in most Prairie basins (Hayashi et al., 2016), due to the presence of aquitards caused by heavy clay till sub-soil deposits (Woo and Rowsell, 1993), and as evidenced by the common lack of base flows in Prairie streams. Niazi et al. (2017) found the average recharge of a small watershed at the western extreme of the Canadian PPR to be 5.3 mm/y by chloride mass balance, and 5–15 mm/y from baseflow estimates, which are very small fractions of the mean annual precipitation of 483 mm. It should be noted that these recharge depths would actually be considered to be quite large in much of the PPR, that the basin in question was not completely underlain by glacial till, and that the depth of the surficial till was very shallow in many parts of the basin (Hayashi and Farrow, 2014). Removals of water from depressions are primarily caused by open water evaporation, transpiration from the surrounding vegetation, and surface outflows when the depressions are filled.

As well as having very different magnitudes, the additive and subtractive fluxes act upon very different areas of the basin. Whilst evaporation and direct precipitation act on the pond surfaces, runoff originates from the uplands surrounding the depression, and blowing snow may be transported from outside of the depression catchment as snow can be blown over drainage divides. Furthermore, addition of water causes ponds to enlarge, and to merge, whilst removal of water causes ponds to disintegrate, and for the smaller ponds to disappear. Shook et al. (2013), and Zhang et al. (2009) demonstrated that the frequency distributions of pond areas change differently when water is added and removed. Therefore the fluxes are not reversible, nor are their effects on the spatial and frequency distributions of pond volumes and areas. Shook et al. (2015) demonstrated that the hysteresis between the storages of water and the connected fractions of Prairie basins was instrumental in affecting the shapes of the probability distribution functions of stream flows.

It is evident that as soon as the elevation of the pond is below that of its depression's outlet, the depression is disconnected as are all depressions upstream. Because evaporation affects all of the ponds in a basin, it is also evident that all depressions will become disconnected at approximately the same time, i.e. as soon as there is evaporation following a runoff event, causing the basin connected fraction to become zero.

Some of the first modelling of the variable connected fractions of Prairie basins was done by Shaw (2009). However, only very small numbers of ponds were examined, and only the increase in the contributing fraction with increasing storage was simulated. Shaw et al. (2012b) examined the increase in contributing area at St. Denis during a runoff event. Shaw et al. (2012a) extended the work to larger numbers of ponds, again for increases in storage and contributing fractions. Shook and Pomeroy (2011) and Shook et al. (2013) extended the work to use many more ponds and larger basins, as well as decreasing storage situations.

### 1.3. Research objectives

The variable connected-fractions are defining state properties of Prairie basins and strongly influence the runoff response to snow melt and precipitation and overall hydrology of the region. Prior modelling research has often been concerned with quantifying the effects of changes in depressional storage on the hydrological responses of Canadian Prairie basins (Ameli and Creed, 2019; Pomeroy et al., 2014).

The objective of this research is to determine the cause of the shapes of the connected-fraction - depression storage volume relationships. It is hypothesized that the relationships are influenced by both the spatial and frequency distributions of depressional storage. The intent is to quantify the effects of both. Three sets of analyses are presented. The first analyses are to determine the effects of the spatial arrangement of depressions on the rising limb of the hysteresis curves. The second analyses determine the influence of the frequency distributions of depressional areas on the curve shape. The third analyses examine the combined effects of the size and location of large depressions.

## 2. Materials and methods

### 2.1. Research locations

The simulations in this study are based on two instrumented and intensively studied prairie pothole basins in Saskatchewan: St. Denis Research Basin (SDRB) and Smith Creek Research Basin (SCRB), whose locations are shown in Fig. 1. The basins have very different topographies and histories and so represent the variability of drainage basins within the PPR. The areas of the sub-basins and the number of depressions (areas $>= 25$ m$^2$) are given in Table 1. Maps of the basins are shown in Fig. 2.

SDRB is located near Saskatoon, SK, and has been studied intensively for more than 30 years. The basin has relatively high relief for the PPR,

**Table 1**
Basin areas, numbers of depressions with areas equal to or greater than 25 m$^2$, areal fractions of depressions, and the fraction of the total depressional area contained in the largest depression, for SDRB and SCRB sub-basins.

| Basin | Sub-basin | Area (km$^2$) | Depressions | Depression area fraction | Areal fraction of largest depression |
|---|---|---|---|---|---|
| SDRB | St. Denis Basin | 22.1 | 2,787 | 0.272 | 0.323 |
| | Brannen Basin | 1.2 | 161 | 0.229 | 0.287 |
| | Basin above pond 90 | 10.3 | 1,445 | 0.212 | 0.282 |
| SCRB | Sub-basin 2 | 51.7 | 11,009 | 0.214 | 0.060 |
| | Sub-basin 3 | 58.4 | 12,372 | 0.227 | 0.033 |
| | Sub-basin 4 | 37.9 | 8,788 | 0.245 | 0.169 |
| | Sub-basin 5 | 11.0 | 2,164 | 0.249 | 0.088 |

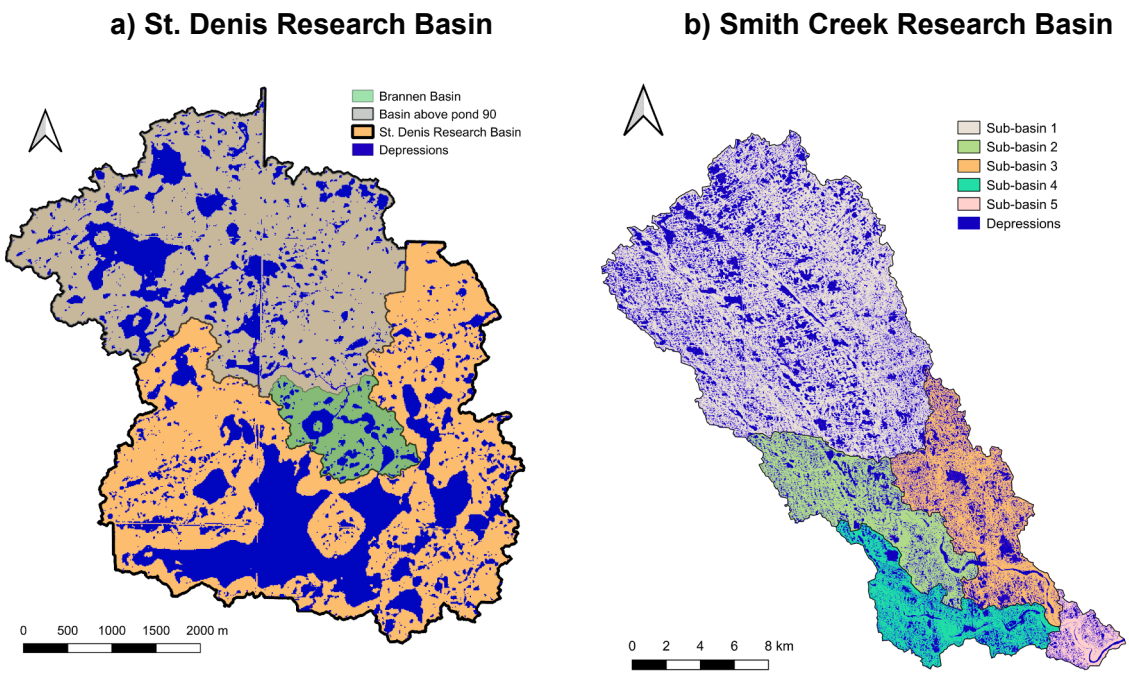


**Fig. 2.** Maps of a) St. Denis Research Basin and b) Smith Creek Research Basin, showing sub-basins. The depression areas are plotted in blue. Projection is UTM 13.

as it is a knob and kettle moraine with slopes varying from 10 to 15% (Miller et al., 1985). The basin has never undergone artificial drainage. The basin is ungauged, which is not surprising as there is no permanent natural drainage system, although some ephemeral channels do exist (Brannen et al., 2015). The entire SDRB lies within the non-effective regions plotted in Fig. 1 and has never been known to discharge flows during the period of study.

The area of SDRB is approximately 22 $km^2$. A LiDAR-based Digital Elevation Model (DEM) is available for the basin. Fig. 2a shows the depression areas (plotted in blue), which were determined using the Wetland DEM Ponding Model (Shook and Pomeroy, 2011), which is described below. Sub-basins may be defined based on the regions draining into the depressions.

SDRB drains from north to south. The larger of the two sub-basins considered in this study is defined as draining into pond 90 and was studied and modelled by Mann (1974). This sub-basin has an area of 10.3 $km^2$, and drains from the overall basin surface divide, to a point just above a very large depression. The smallest basin was studied by Brannen (2015) and Brannen et al. (2015), so it is designated as "Brannen Basin". The total area of the sub-basin is approximately 1.2 $km^2$ (Brannen et al., 2015). Brannen Basin differs from the other two basins as it does not include the headwaters, and therefore can receive discharges from upstream. Note that the outlet of Brannen Basin is the same as that of the basin draining into pond 90.

SCRB is a low-relief basin in southeastern Saskatchewan, with a gross drainage area of approximately is 400 $km^2$, and slopes between 2 and 5% (Pomeroy et al., 2014). Unlike SDRB, SCRB has a conventional drainage system with a stream gauge operated by the Water Service of Canada (WSC), 05ME007 SMITH CREEK NEAR MARCHWELL, which has been operational since 1975. Approximately 87% of the basin was classified as being non-effective by the Prairie Farm Rehabilitation Administration (PFRA) (Government of Government of Canada, 2013).

SCRB has been drained very extensively since at least 1958 (Dumanski et al., 2015), and has been studied extensively and modelled by the Centre for Hydrology since 2008 (Brunet and Westbrook, 2012; Fang et al., 2010; Minke and Westbrook, 2010; Minke et al., 2010; Pomeroy et al., 2014; Shook et al., 2013). LiDAR taken in 2008 showed more than 10,000 depressions having areas greater than 100 $m^2$, although the number and sizes of the depressions have since been reduced by drainage. Fig. 2b shows the arrangement of sub-basins within the basin, as well as the depression areas determined from the LiDAR DEM using ArcGIS as described by Pomeroy et al. (2014). Because the execution time was too large, WDPM (described below) was not run for Sub-basin 1, although the model was run successfully for Sub-basins 2 through 5. The basin drains from north-west to south-east, i.e. from Sub-basin 1 to Sub-basin 5.

### 2.2. Models

Two models, the Wetland Digital Elevation Model (DEM) Ponding Model (WDPM), and the Pothole Cascade Model (PCM), are used in this study. In this study, the models apply spatially uniform fluxes of water to representations of depressional storage in Prairie basins. Although actual fluxes greatly vary in both space and time, the intent of the study is to determine the how the geometry of depressional storage affects the responses of Prairie basins.

#### 2.2.1. The wetland digital elevation model (DEM) ponding model (WDPM)

Shook and Pomeroy (2011) and Shook et al. (2013) developed the WDPM which applies water to a DEM, and routes the flow overland using the algorithm of Shapiro and Westervelt (1992). The WDPM source code is available at https://github.com/CentreForHydrology/WDPM. Compiled versions of the model, and more supporting documentation, are available at https://research-groups.usask.ca/hydrology/modelling/wdpm.php. The model has been used by several researchers other than the authors to simulate the variable spatial distributions of water within prairie basins (Kiss, 2018; Schellenberg, 2017; Thapa et al., 2019).

WDPM can be used to estimate the connected fraction of a basin having any state of distribution of water. A small depth of water (1 mm) is added, and the basin is drained. The fraction of the applied depth of water which exits the model is therefore the fraction of the basin which is connected to the outlet.

As shown in Fig. 3, when run repeatedly for a prairie basin, WDPM

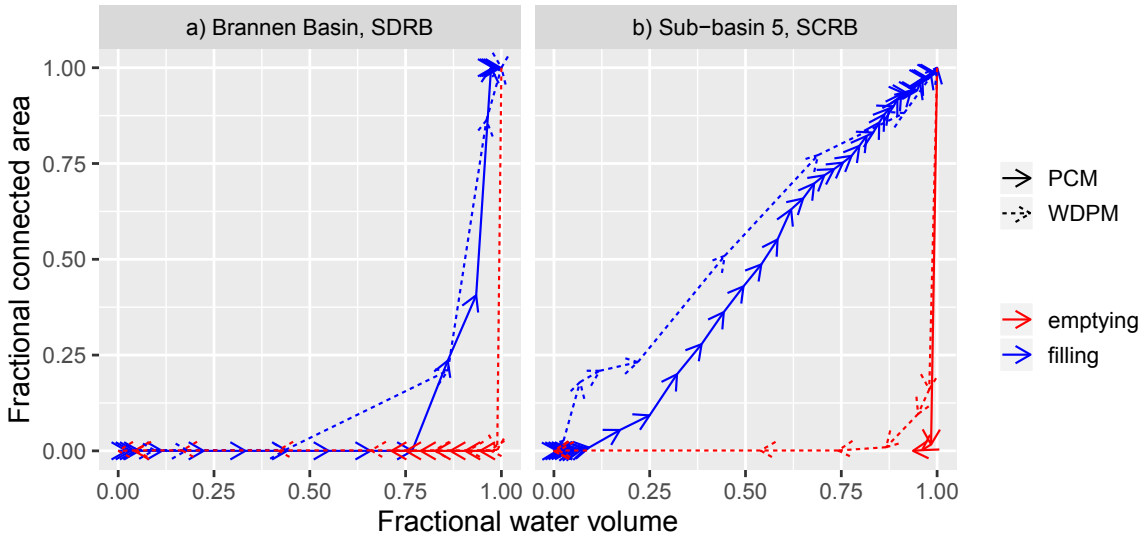


**Fig. 3.** Fractional connected area hysteresis loops simulated by WDPM and PCM for a) Brannen Basin, St. Denis Research Basin and b) Sub-basin 5, Smith Creek Research Basin.

produces hysteresis loops between the connected fraction, and the volume of water storage. The plotted loops are for complete filling of the storage from the initially-empty state, followed by complete removal of water. The hysteresis loops could not be verified experimentally, but the changes in the frequency distributions of water areas produced by the model have been validated against remotely sensed water areas by Shook et al. (2013) and Armstrong et al. (2013).

WDPM was used to determine the sizes of depressions in all of the sub-basins examined by repeatedly adding simulated water, until the basins were filled. In all cases LiDAR-derived DEMs with resolutions of 5 m were used. WDPM simulations showed that SDRB has approximately 126 depression per km$^2$; the mean value for SCRB is 216. Given that the total areal fraction of all depressions is slightly greater in SDRB, the mean depression area is also greater in SDRB than in SCRB. Table 1 also shows the depressional area fraction, i.e. the fraction of each basin within depressions. St. Denis Basin has a much greater fraction of its area (0.272) as depressions than any other basin.

### 2.2.2. The pothole cascade model (PCM)

Because WDPM is too slow and inflexible (it cannot easily simulate changes in drainage) to be a component of a hydrological model, the simplified conceptual PCM was developed. The PCM source code and documentation are available at https://github.com/CentreForHydrology/PCM. PCM applies spatially uniform fluxes to a set of model depressions, which are selected to have similar volume-area scaling properties, frequency distributions, and patterns of connection, to those in the basin being simulated (Shook et al., 2013). PCM is similar to the model of Shaw (2009), which also applies fluxes to simulated depressions; however PCM is much faster, allowing the use of much larger numbers of depressions and also simulates the removal of water from the depressions. Although PCM cannot reproduce the aggregation and disaggregation of ponds, it does simulate the connection and disconnection of depressional areas, and produced connected fraction – volume fraction hysteresis loops with shapes similar to those produced by WDPM, as are shown in Fig. 3. The addition of the PCM algorithm to a physically-based hydrological model of SCRB was shown to dramatically improve the model's performance (Pomeroy et al., 2014).

Unfortunately, the PCM algorithm is difficult to use in practice. As PCM requires each pond to be represented, it dramatically increases the number of parameters and state variables required by a model. Mapping the connectivities of large numbers of depressions in a basin is very difficult. Pomeroy et al. (2014) simplified this task by only using a small number of depressions (46) to represent all of the depressions in each sub-basin of SCRB. The effects of using small numbers of simulated depressions were identified by Shook and Pomeroy (2011), but were not well quantified.

PCM is used in this research to investigate the effects of the arrangement of depressional storage on the hysteresis between water storage and the fraction of the basin which is connected to the outlet. The model's parametric requirements are modest, consisting of simple text files listing a) the volume b) the area and c) the connectivity, i.e. the draining destination, of each depression. The catchment area of each depression is computed from the depressional area as described below.

The area ($A_p$, m$^2$) and volume ($V_p$, m$^3$) of each pond are modelled as paraboloids using the relationships of Hayashi and van der Kamp (2000):

$$A_p = sh^{\frac{2}{p}}, \tag{1}$$

where s, p = constants, h = pond maximum depth (m).

Therefore the volume of a pond is function of its surface area

$$V_p = A_p \frac{h}{\left(1+\frac{2}{p}\right)}. \tag{2}$$

Hayashi and van der Kamp (2000) found great variation in the values of s and p among depressions in several Prairie basins. All PCM simulations used values of p = 1.72 for ponds with depressions smaller than 10,000 m$^2$, and p = 3.33 for the larger ones, which were used by Pomeroy et al. (2014), and were derived for SCRB. Although these values provide some representation of the effect of depression area on p (and therefore h), they do not reproduce all of the scaling, nor the natural variability in the parameters.

Based on the assigned value of p, and the depression area and volume, the values of s and h were computed for each depression, by iteratively solving Eqs. 1 and 2. The depression areas were determined by GIS analyses of Smith Creek Sub-basin 5, as described in [Pomeroy et al. (2014).

Shook et al. (2013) found power-law relationships between the areas of depressions ($A_d$, m$^2$) and their catchments ($A_c$, m$^2$):

$$A_c = aA_d^b, \tag{3}$$

where a and b are constants; the magnitudes of b being less than 1 for the three Prairie basins examined. For Smith Creek Sub-basin 5, a = 31.3, b

= 0.738. This relationship was used to calculate the catchment area for each depression simulated.

The depression volumes ($V_d$, $m^3$) at SCRB were found to fit a power-law relationship with the depression areas, as was also described in (Pomeroy et al., 2014):

$$V_d = cA_d^d, \quad (4)$$

where d = 1.211.

As the volume and catchment area of a given depression are functions of its area, it is usually easier to estimate the relative size (and therefore importance) of a depression from its area than from the volume. Therefore areas provide a convenient way of categorizing depressions.

Because the exponent of Eq. 4 is greater than 1, and that of Eq. 3 is less than 1, the depression volume increases more rapidly than does the area, while the catchment area increases more slowly. The implications of these scaling relationships are discussed below.

The model forcings are spatially-uniform additions and removal of water. PCM uses a constant factor (in this case set to 1, so as to give the maximum possible connected fractions) to calculate the runoff from the depression and its catchment. Each addition of water is applied to all the depressions. When a depression is filled, any excess water is routed to the specified connecting depression, and to all subsequent connected depressions. When a depression is not full, the connection with the downstream depression is broken, so no water is routed. As with WDPM, the connected fractions of the simulated basins were determined by adding 1 mm of water, and calculating the fraction of water exiting the model.

Each execution of PCM only applies a single depth of water (addition or removal) to the set of depressions. As is discussed below, the PCM simulations required many executions of the program. Scripts written in the language **R** (R Core Team, 2013) were used to create the parameter files and to repeatedly call the PCM executable. All the **R** scripts and associated data files used in this document are available through Zenodo (https://zenodo.org/record/3964953#.X-n6z3VueV6).

### 2.3. Mapping depressional spatial distributions

Determining the effects of the spatial distribution of storage requires methods of quantifying it. Phillips et al. (2011) used network analyses to map the connectivity of lakes in northern Canada, which share some similarity with the PPR in that both regions are flat and poorly drained. Rains et al. (2015) used network graphing to describe the arrangement of GIWs.

Herein, network graphs are plotted of the arrangement of depressions as shown in Fig. 4, with the depressions as the vertices, and the potential overland flow connections as the edges. All network graphs in this paper are plotted using the R package *igraph* (Csardi and Nepusz, 2006). The outlet from a given basin is represented by the red vertex in each plot.

The spatial arrangement of depressional storage was quantified using a variation of the basin width function, which quantifies the number of tributary streams as a function of the flow distance from the outlet. The basin width function has been linked to the shape of basin hydrographs by researchers since Kirkby (1976). When applied to depressional storage, the width function is simply the histogram of the number of depressions (vertices) versus their distance (in edges) from the outlet. In a basin where many depressions are located near the outlet (i.e. where water does not have to flow through many depressions to reach it), the width function will be skewed rightward. If many depressions are located near the outer reaches of the basin, the function will be skewed leftward. If many depressions are located in the middle of the basin, with

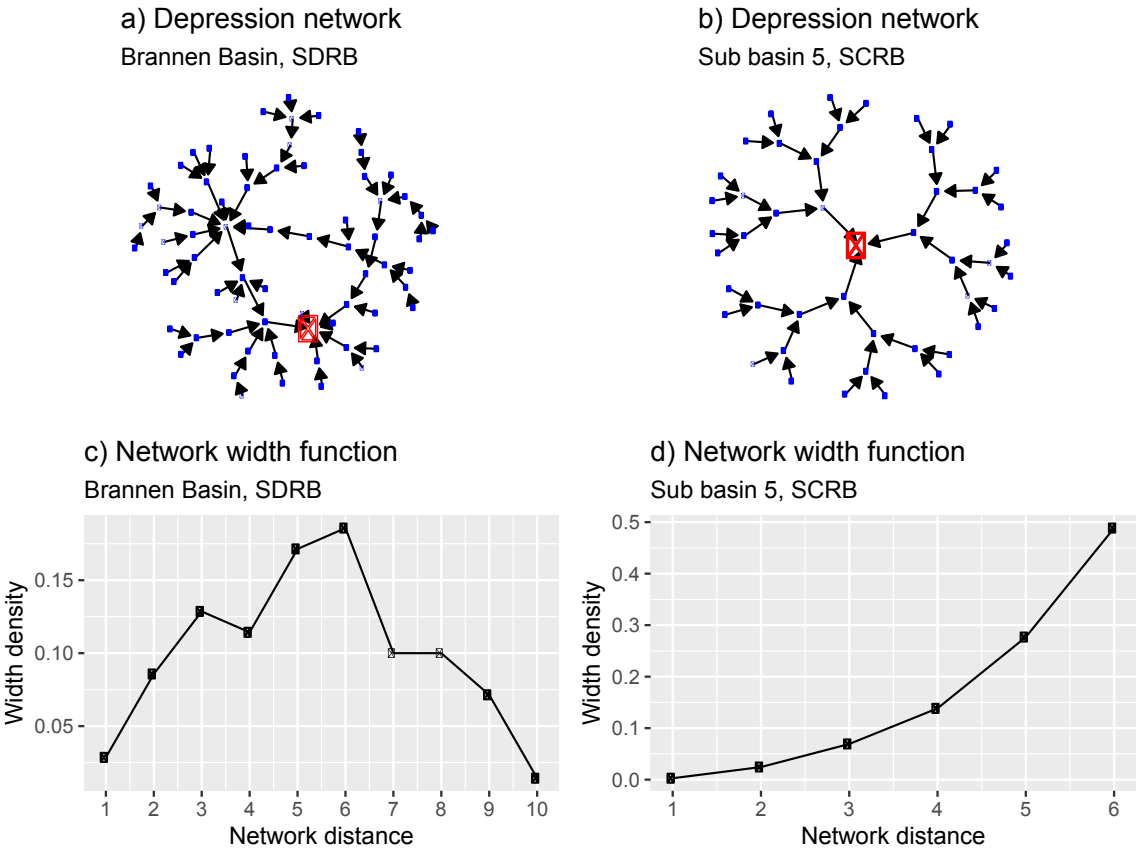


**Fig. 4.** Depression graphs (a, b) and width functions (c, d) for Brannen Basin and SCRB Sub-basin 5. The outlets of the graphs are the large red nodes. All other depression nodes are small and blue. The width functions are histograms of the density of depressions vs. distance from the outlet.

few near the outlet and in the outer reaches of the basin, then the width function will be heap-shaped. To allow comparison among basins with varying numbers of depressions, the widths are converted to densities by dividing by the total numbers of depressions in the basins.

The graph of the depressions at Brannen Basin, SDRB is plotted in Fig. 4a; their arrangement appears to be quite random. As shown by Shook and Pomeroy (2011), the depressions in each sub-basin at SCRB are arranged in "tributaries" that drain in parallel to the stream channel. Therefore, all tributary sets of depressions in this basin can be regarded as draining directly to the outlet. It is believed that the structured arrangement of the "tributaries" is due in part to the high degree of artificial drainage in the basin (Dumanski et al., 2015). The minimum number of depressions that could represent the connectivity estimated for this basin is 46, as described in Pomeroy et al. (2014), arranged as shown in Fig. 4b.

As discussed by Phillips et al. (2011) in the context of lakes in northern Canada, large depressions act as "gatekeepers" preventing upstream flows from contributing to the outlet until the large depressions are filled. The filling curve for Brannen Basin, plotted in Fig. 3a strongly resembles the filling curve plotted by Shaw et al. (2012a) in their Fig. 6c, which shows a small sub-basin dominated by the gatekeeping of a single large depression at the outlet.

The network width function of Brannen Basin, plotted in Fig. 4c, indicates that the largest fractions of depressions are located near the middle of the basin. However, the spatial distribution of depressional maximum water areas, plotted in Fig. 5a, shows that there are several large depressions located very close to the outlet, which cause the gatekeeping function seen in the plots in Fig. 3a, where the connected area fraction is zero until approximately 75% of the depressional storage has been filled. Apart from these large depressions, there does not appear to be any relationship between the sizes and the network locations of the depressions.

The network width function of SCRB Sub-basin 5, plotted in Fig. 4d, shows that most of the depressions are located far from the outlet, as would be expected from a branching arrangement. The plot of depressional area vs. network distance for SCRB in Fig. 5b show little relationship between the size of a depression and its location within the basin – the location is essentially random. In this case, the depression locations are indexed by the Horton-Strahler order of an overlaid drainage network, as described in (Pomeroy et al., 2014), which is another measure of the network distance. The Horton-Strahler order was used because of the difficulty in identifying the connectivities of a very large number of depressions.

The filling curves for SCRB Sub-basin 5 plotted in Fig. 2b, are very linear, rather than showing the "stair step" arrangement of the curves in Fig. 6 of Shaw et al. (2012a). The number of depressions used in a PCM simulation has been demonstrated to strongly affect the smoothness of the filling curve (Shook et al., 2013). Therefore, it is very likely that some of the difference between the shapes of the filling curves at SDRB and SCRB is due to the difference in the numbers of depressions in the basins.

### 2.3.1. *Modelling the effects of depression arrangement*

The effects of the frequency and spatial distributions of depressions on the shapes of the filling curves were investigated by generating synthetic networks of depressions, and then using PCM to find the connected fractions as the networks were filled. Synthetic networks allow the depressions to be in any desired arrangement, allowing realistic or completely artificial networks.

The effects of the number and spatial distribution of depressions on the shapes of the filling curves were investigated by generating synthetic networks of depressions, and then using PCM to find the connected fractions as the networks were filled. Networks were created with 46, 92, 184, 368, and 736 depressions, i.e. 1, 2, 4, 8 and 16 sets of 46

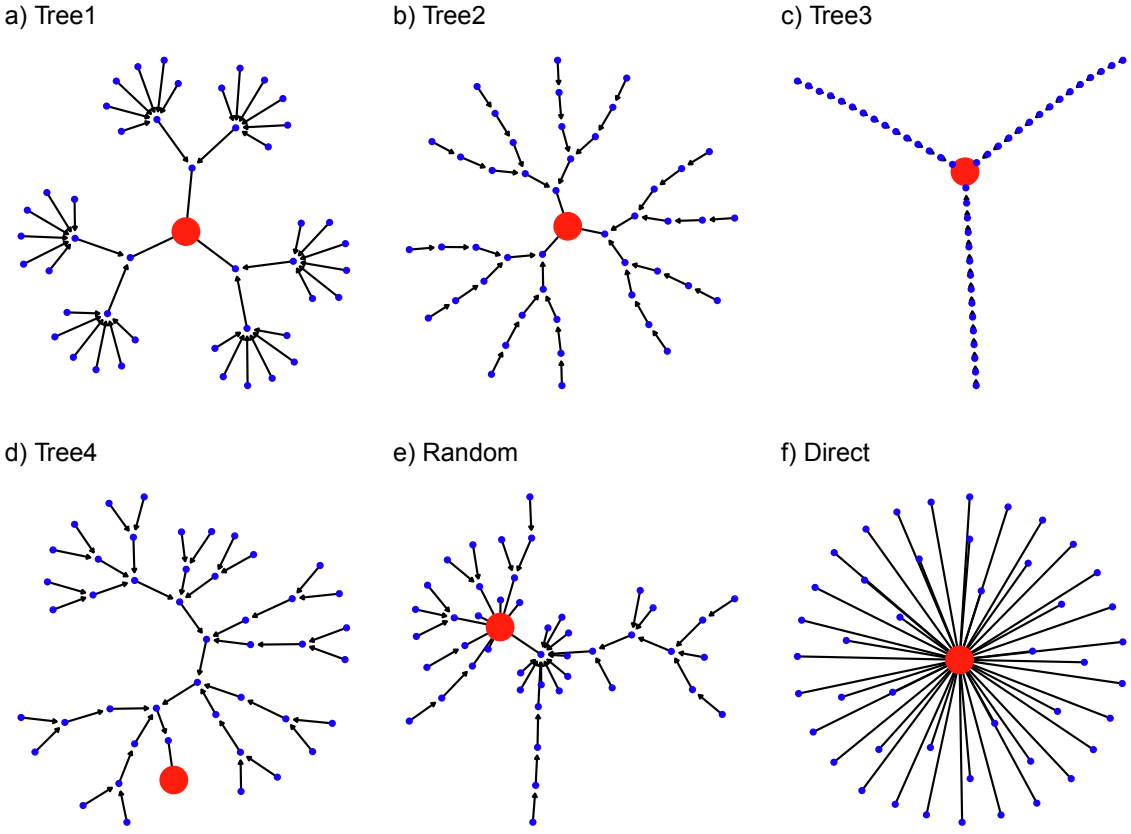


**Fig. 6.** Graphs of synthetic networks. The outlet of each network is the large red node, all other depression nodes are small and blue. The arrows (edges) indicate the connectivity of each depression node.

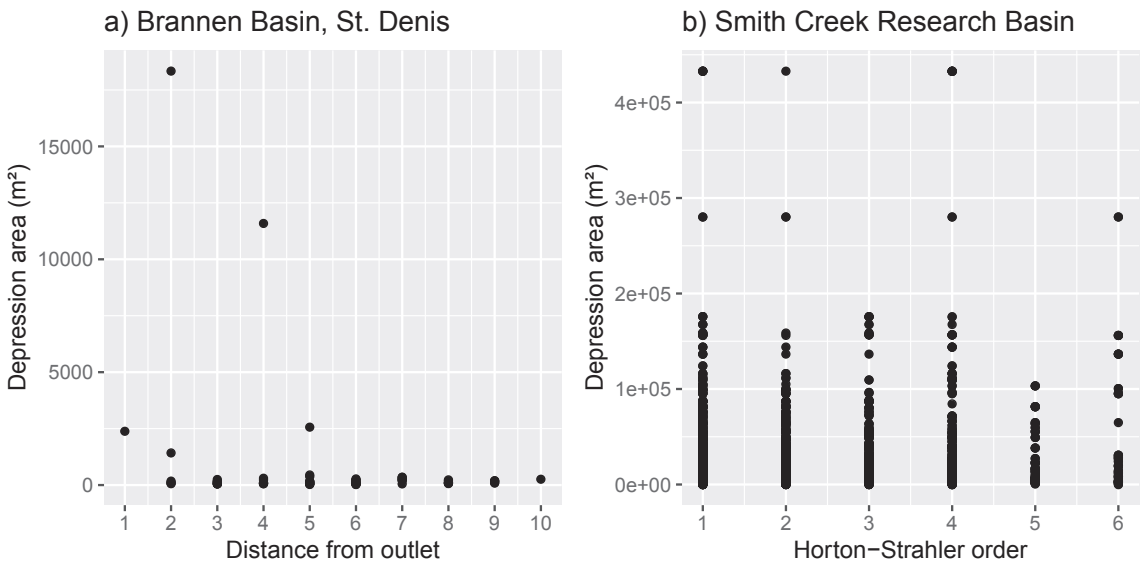


**Fig. 5.** Depression area vs network distance from outlet for a) Brannen Basin and b) SCRB. The SCRB distances are the Horton-Strahler orders for an overlaid drainage network.

depressions (as was used by the original PCM model for SCRB) for each of the network arrangements. Each set of 46 depressions was connected separately to the outlet, giving the complete set the same width function as the original 46 depressions.

Three types of storage network graphs were simulated: 1) deterministic, 2) random, and 3) direct. The deterministic graphs use sets of 46 depressions in 4 tree-based arrangements, shown in Fig. 6a–d. The network width functions of these basins plotted in Fig. 7 a through d place the depressions at varying distances from the outlet. The **Tree1** network is distributed very similarly to the SCRB network with the depression density rapidly increasing with network distance. The density plots of networks **Tree2** and **Tree4** show that these networks are intermediate between the distributions of the SCRB Sub-basin5 and Brannen Basin. The **Tree3** network was created as a test of an extreme example of gatekeeping; it is not intended to be realistic representation of a Prairie basin.

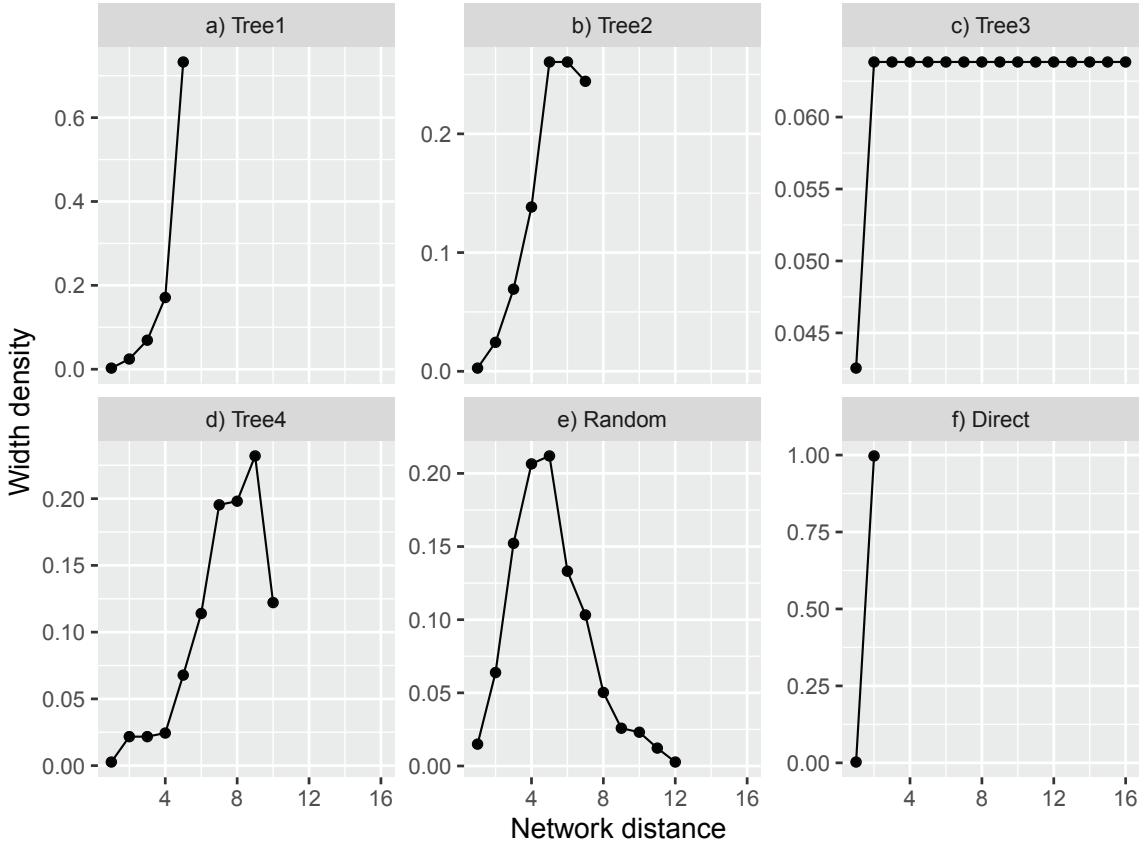


**Fig. 7.** Width functions (histograms of the density of depressions vs. distance from the outlet) of synthetic networks.

The **Random** graphs were generated using the R *igraph* package function `sample_pa`. Varying the power parameter of the function allows the creation of graphs of varying sizes, with very similar network width functions.

Fig. 6e plots the network generated for 46 depressions. As plotted in Fig. 7e, the network width density indicates that this method places a large fraction of the depressions adjacent to the middle of the basin, similar to the distribution of Brannen Basin.

The **Direct** network, plotted in Fig. 6f, connects each depression directly to the outlet. There are no connections among the depressions, so no depression can perform gatekeeping of upstream depressions. Therefore, as plotted in Fig. 7f, all of the depressions (other than the outlet) have the same distance from the outlet.

As the spatial distributions of depression areas at SDRB and SCRB are generally random, as shown in Fig. 5, the depression volumes and areas were distributed randomly among the networks. Twenty realizations were created for each of the networks, i.e. the same set of depression parameters was assigned randomly over each model network 20 times.

The sequence of operations for modelling was:

1. A set of depressions was selected with either 46, 92, 184, 368, or 736 depressions, i.e. with 1, 2, 4, 8 or 16 sets of 46 depressions.
2. An arrangement pattern was selected from the 6 depressional arrangement patterns ("Tree1", "Tree2", "Tree3", "Tree4", "Random" and "Direct").
3. The depressions were assigned randomly to all positions in the arrangement.
4. A small depth of water was added to the depressions and all of their catchments, and allowed to run into the depressions or to exit the model.
5. An additional 1 mm of water was added to the model, and the fraction of the applied depth exiting the model was recorded as the connected fraction.
6. Steps 4 and 5 were repeated until all of the model depressions were filled, and the connected fraction of the simulated basin was 1. Together, 118 additions of water were made: additions of 1 through 10 mm were added by 1 mm, followed by additions of 20 through 500 mm, by 10 mm, for a total of 59 additions, followed by 59 additions of 1 mm.
7. Steps 3 through 6 were repeated with 20 different realizations of the random arrangement of the model depressions.
8. Steps 2 though 7 were repeated for all 6 depressional arrangement patterns.
9. Steps 1 through 8 were repeated for all 5 numbers of depressions.

Steps 4 and 5 were performed by PCM. All of the other steps were performed by **R** scripts which called the PCM model. In total, 70,800 PCM runs were made: 118 additions of water × 5 sets of depressions × 6 arrangement patterns × 20 realizations.

### 2.4. Frequency distributions of depression areas

As described above, it is believed that the frequency distribution of depression areas (and therefore of their volumes and catchment areas) influences the shapes of the connected-fraction curves. It would appear that the area frequency distribution within a given basin has two important components, a) the frequency distributions of all depressions, and b) the relative sizes of the largest depressions, which strongly gatekeep. It is therefore important to determine the effects of both components.

Several researchers have found that pond areas, and therefore presumably depression areas, can be approximated by power-law frequency distributions (Liu and Schwartz, 2011; Shook et al., 2013; Zhang et al., 2009), which is common in objects, such as depressions, which are fractals (Bertassello et al., 2018; Minke et al., 2010). Mekonnen et al. (2014) demonstrated that integration of an assumed power-law distribution of depressional volumes could produce single-valued exponential curves for the contributing fractions of Prairie basins. When the algorithm (PDMROF), was employed for basins within the Canadian PPR, it improved the performance of the hydrological models (Mekonnen et al., 2014; Mengistu and Spence, 2016). However PDMROF does not explain the shapes of the hysteretic curves plotted in Fig. 3, as it produces a single-valued function, and PDMROF uses calibrated parameters, rather than actual frequency distributions. PDMROF also uses an assumed continuous distribution, rather than discrete depressions. Most importantly, PDMROF does not use a relationship between pond areas and volumes, nor a relationship between the depression and catchment areas.

Pareto II distributions were fitted to all of the to all of the SDRB and SDRB depressional areas, using the R package *CoSMoS* (Papalexiou and Serinaldi, 2020; Papalexiou et al., 2020), which is available at https://cran.r-project.org/package=CoSMoS. Sets of between 10 and 20,000 depressions, with 10,000 realizations of each set, were generated from the fitted distributions. Realizations resulting in maximum fractional depression areas greater than the maxima of the values for SDRB and SCRB were eliminated. In all cases more than 8,900 realizations were used for each set of depressions.

The areal fractions of the largest depressions are plotted against the number of depressions in each set in Fig. 8 for all of the sub-basins at SDRB and SCRB. For both basins, the median areal fraction decreases rapidly, becoming fairly flat for sets of more than 5000 depressions, with the SCRB median values being consistently smaller than the SDRB values.

The measured values of the largest depression areal fractions, plotted as red dots, are much greater at SDRB than at SCRB. This is only partly due to the small numbers of depressions at SDRB; SDRB has more depressions than SCRB Sub-basin 5, as is shown in Table 1. Evidently the size distribution of depression areas at SDRB also results in relatively large values of the areal fractions. Therefore, the relative area of the largest depression will depend on the size of the basin, and the overall frequency distribution of depression areas, as well as random chance.

#### 2.4.1. Modelling the effects of the depression area frequency distribution

The cause of the near-linear rising-limb connected-area curves plotted in Fig. 3b for Sub-basin 5, SCRB were investigated by filling sets of simulated depressions with similar properties. In these simulations the filling of each set of depressions was effected by an R script which iteratively applied depths of water to the depressions and their catchments, until all of the depressions were filled. The simulation was therefore very similar to those of the **Direct** PCM simulations in that each depression was assumed to be connected to the outlet as soon as it was filled.

As demonstrated by Eq. (3), the relationships between the areas of depressions and their catchments can be described by power-laws, although Shook et al. (2013) showed that the relationships have considerable scatter, particularly for small depressions. Depression basins were modelled by generating a bivarate copula from the fitted marginal distributions of the areas of the depressions and their catchments, using the **R** packages *copula* (Hofert et al., 2018) and *VineCopula* (Nagler et al., 2019).

Using the copula for SCRB Sub-basin 5, 10,000 sets of 1,000 random depressions were drawn. Each set was selected to have the same maximum and minimum depression sizes as the original SCRB Sub-basin 5 depressions, and the total depressional area fraction was limited to that of the sub-basin. The volumes of the ponds were estimated from their areas, using Eq. 4. Thus each set of simulated depressions and their catchments represents a random realization of a basin. The median value of the areal fraction of the largest depression for each set of depressions was 0.053.

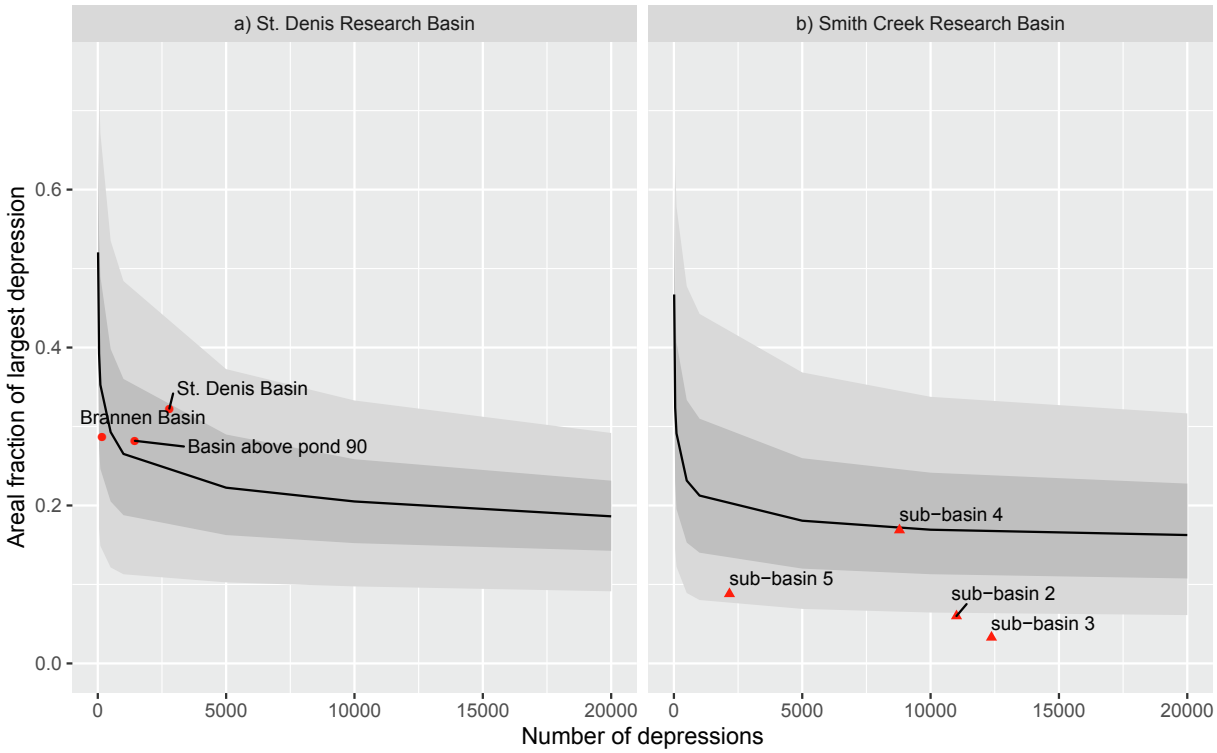


**Fig. 8.** The fraction of the total depressional area occupied by the largest depression vs. the number of depressions for a) St. Denis Basin and b) Smith Creek Research Basin. The line represents the median value as determined by sampling fitted Pareto II distributions. The light gray shaded region defines the 5% and 95% quantiles, the dark gray shaded region defines the upper and lower quartiles. The red circular and triangular points plot actual values for SDRB and SCRB, respectively.

### *2.5. Simulating depression frequencies and arrangements*

To quantify the combined effects of the depression area and location on gatekeeping, a set of PCM models was executed which incorporated both variables. Each model consisted of 2,944 depressions arranged in 4 branches of 736 depressions, each branch using the **Tree1** arrangement. For each model run, a single large depression was generated with an area between 0.02 and 0.3 of the total depressional area. The largest depression was sited within the network, so that between 0.125 and all of the total basin area (other than that of the depression) was located above it.

## 3. Results

### *3.1. Depression arrangement simulations*

As described above, sets of depressions were connected in the 6 arrangements plotted in Fig. 6. Each set of depressions was filled from the initially empty state, to the completely filled state, using PCM.

The first set of PCM model runs, as plotted in Fig. 9, was for sets of 46 depressions. The filling curves for the networks of 46 depressions all show strong signs of stair steps. Much of this effect is due to gatekeeping, as the sizes and locations of the steps vary among the networks, the strongest effects being for the **Tree3** and **Tree4** networks. However, the plot for the **Direct** network, which does not have downstream gatekeeping, also shows stair steps. In this case, the stair steps are due to the filling of large depressions, which only perform gatekeeping for themselves.

There is considerable variability among the curves in Fig. 9 for each network, except for the Direct network, where all runs produce the same curve because the network location is always the same for all depressions in all runs. Note that two of the curves for the **Tree4** network are similar to the filling curve for Brannen basin plotted in Fig. 3a, showing zero connected fraction until a large fraction of the total depressional storage was filled.

The filling curves for the set of PCM model runs using sets of 736 depressions, plotted in Fig. 10, show greatly reduced stair steps and the curves are much more similar to each other, both within a given network type and between network types, than are the 46-depression curves. As with the 46-depression curves, the **Direct** network produces a single curve, regardless of the assignment of depressions. The cause of the reduced magnitudes of the stair steps is undoubtedly that the fraction of the total depressional storage held in any single depression is reduced as the number of depressions is increased.

The 736-depression filling curves approach 1:1 lines, regardless of the shape of the network, similar to the plots for SCRB Sub-basin5 in Fig. 3b. The differences in between the filling curves and a 1:1 line were quantified by computing the root mean squared difference (RMSD) between the each filling curve and the 1:1 line.

Fig. 11a plots the median value (averaged over all realizations) of RMSD for each network type, for 46, 92, 184, 368 and 736 depressions. The shaded regions represent the upper and lower quartiles of RMSD for the 20 realizations. The plot shows that the median value of RMSD decreases for all network types, as the number of depressions increases. In all cases the median RMSD value was smallest for the **Direct** network type, and was the largest for the **Tree3** network type, as would be expected.

Although the variability in RMSD is influenced by the network structure, it appears that the number of depressions has a much greater effect. Fig. 11b plots the fraction of the total depressional area contained by the largest depression vs. the number of depressions. The value of the area fraction decreases with increasing numbers of depressions, in a very similar way to the RMSD, and very similarly to the results of the simulations plotted in Fig. 8.

### *3.2. Depression area frequency distribution simulations*

Fig. 12 plots the curves of fractional connected area vs. fractional

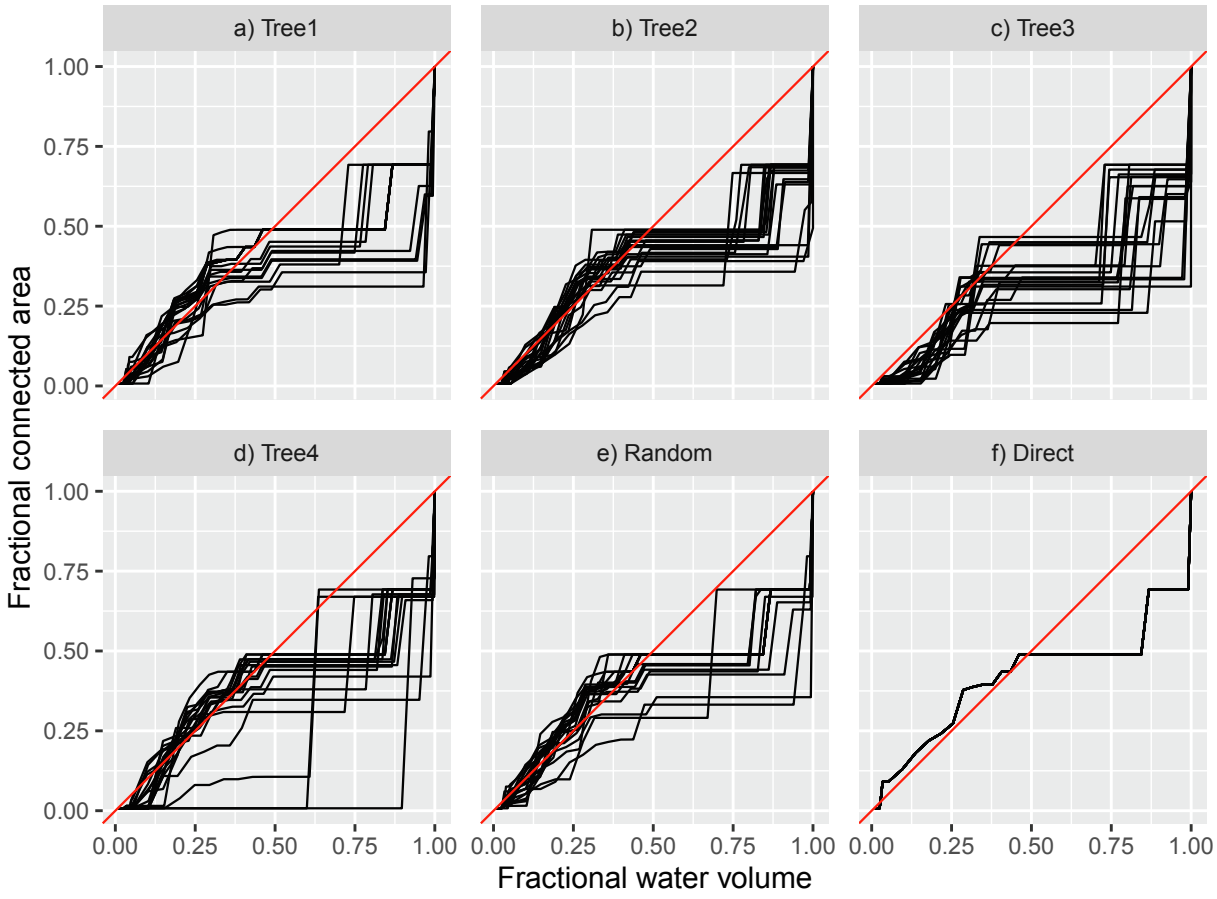


**Fig. 9.** Rising limb envelope curves of fractional connected area vs. fractional water volume, for synthetic networks of 46 depressions, using 20 realizations of depression location. 1:1 lines are plotted in red.

depressional storage for all of the realizations in gray. The median value is plotted in black; a 1:1 line is plotted in red. Although there is considerable scatter, the realization curves lie close to the 1:1 line. The median curve is slightly sigmoidal, rather than being as linear in the curves in Fig. 3b, or the simulations in Fig. 10f. As both sets of simulations used the same relationships for determining pond areas and volumes, it is believed that the cause of the deviation of the curves in Fig. 12 lies in a) the use of a fitted distribution for the depression areas and b) in the use of the very simple scaling relationship of Eq. (4) for the depressional volumes, as well as the use of only 2 values for the parameter p by the second set of simulations.

As the curves in Fig. 12 were generated from only the frequency distributions of depression and catchment areas, and the relationship between depression volumes and areas, it is concluded that the shape of the rising limb of the linear filling curves in Fig. 3b is primarily due to these relationships.

### 3.3. Combined effects of depression size and location

Fig. 13 plots the results of the PCM simulations of a single large depression, of varying size, located at varying locations within a depression network. When the areal fraction of the largest depression is very small its gatekeeping is also small, and therefore its location within the basin is unimportant. As the depression's areal fraction is increased, the effects of gatekeeping are seen most dramatically when it is located at the bottom of the basin, where it causes an initial pause in the connected fraction. As the depression's areal fraction reaches 0.3 of the total area, the pause length increases until the system becomes very nearly endorheic. As the large depression is moved farther up the basin, its effect on the connected-fraction curve changes. The initial pause in connected fraction is shifted upward from the x-axis, as the region downstream of the largest depression becomes connected before the large depression is filled. The rate of filling the downstream depressions is also reduced by the gatekeeping action of the large depression. When the fraction of the basin area above the large depression is 0.15 or less, the large depression is unable to fill, even with the addition of 700 mm of water, because of the very small fraction of the basin above the contributing inflow.

As was described above, the drainage area of a depression is a power-law function of the maximum water area with scaling exponents smaller than 1 (Shook et al., 2013). Therefore the ratio of the catchment area to depression area decreases as the depression area increases, reducing the depths of runoff inflows. When the areal fraction of the largest depression was 0.3, the volume fraction of the depression exceeded 0.5 of the total, so it is able to trap almost all of the water being produced upstream, when it is located near the bottom of the basin. However, the catchment area fraction was less than 0.1 of its depression's area. Therefore, it is difficult for a large depression to fill when it is located near the top of the basin, as it receives water from a small area.

It should be noted that the results above are only for a single set of depressions, using a single large depression, and a particular arrangement (**Tree1**). As scaling Eqs. 3 and 4 are functions of the depression area, the gatekeeping of the maximum depression area will depend on the size of the largest depression, as well as its fraction of the total depressional area. Because only 736 depressions were used on each branch, the simulation likely exaggerates the gatekeeping for small maximum depression areal fractions as other depressions have similar areas to the largest depression.

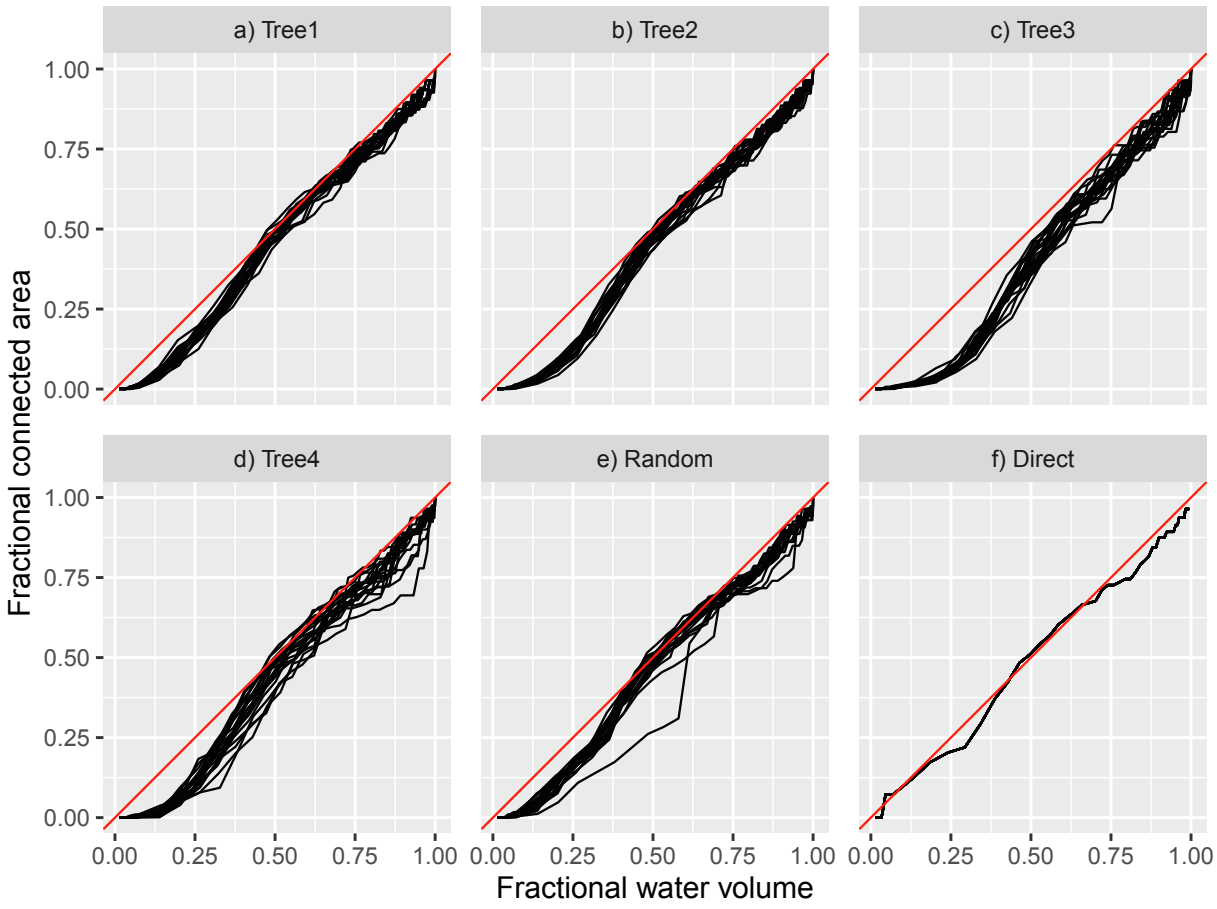


**Fig. 10.** Rising limb envelope curves of fractional connected area vs. fractional water volume, for synthetic networks of 736 depressions, using 20 realizations of depression location. 1:1 lines are plotted in red.

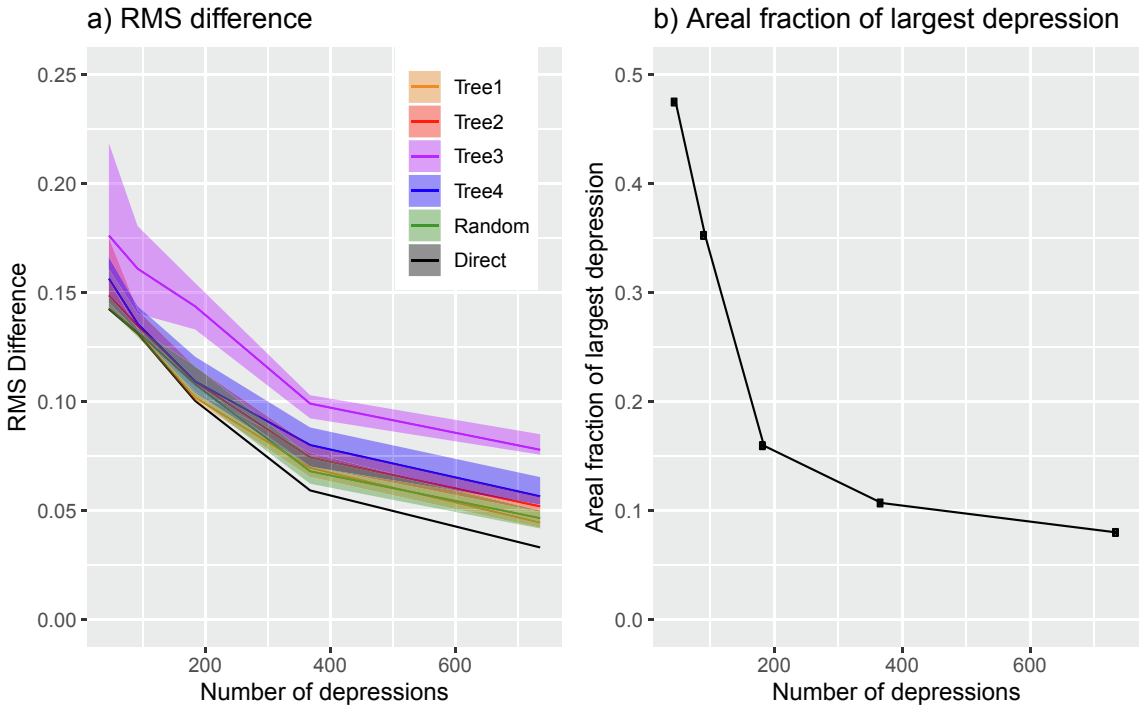


**Fig. 11.** The effect of the number of depressions on a) the RMS difference between the fractional connected area and a 1:1 line and b) the areal fraction of the largest depression. The lines in a) represent the median RMSD, the shaded regions represent the upper and lower quartiles for 20 realizations.

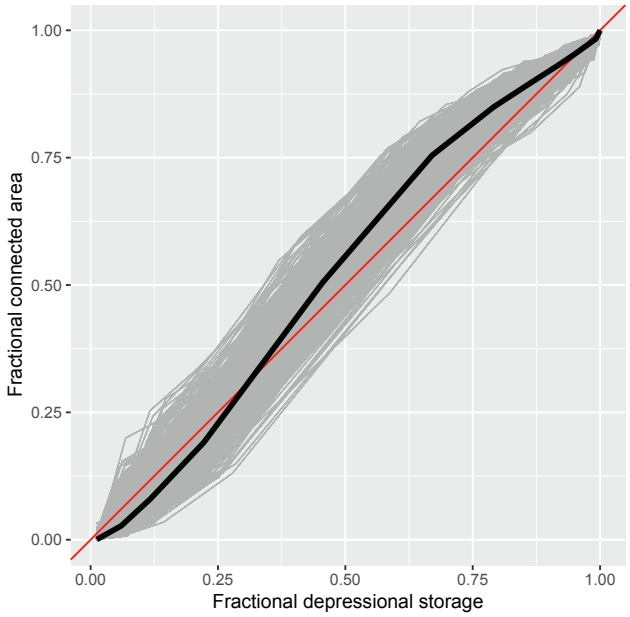


**Fig. 12.** Fractional connected area vs. depressional storage for 10,000 simulations of 1,000 randomly generated synthetic depressions. The individual simulations are plotted in light gray. The heavy black line is the median curve. A 1:1 line is plotted in red.

## 4. Conclusions

Numerical experiments on the fill and spill runoff response for the hydrology of prairie basins with differing networks of depressions show the role of these networks in governing basin hydrological responses.

For basins with small numbers of depressions, the sizes and the spatial arrangement of the depressions are very important in governing the gatekeeping, and therefore the connected fraction of the basin.

For basins with large numbers of depressions, provided that the largest depressions are fairly small, the spatial arrangement of the depressions is relatively unimportant. Where there is a single large depression (i.e. a lake) near the outlet of the basin, the basin may effectively be endorheic, i.e. unable to ever contribute flow downstream. A single large depression near the top of a basin may never contribute flow to the rest of the basin.

The frequency distributions of depression areas in a basin depends on the topography, as well as the existence of artificial drainage. Artificial drainage may also influence the connectivity of the depressions.

The convergence of the basin connected-fraction curves toward 1:1 lines, indicates that the gatekeeping effects of small ponds are also small. The shape of connected fraction curve is largely due to the frequency distribution of depression areas, the relationship between depression area and volume and the relationship between the depression areas and the areas of their catchments.

Small basins, where the arrangement of the depressions is important, and where the depressional area is most concentrated in a single depression, will require detailed modelling using models like WDPM or PCM.

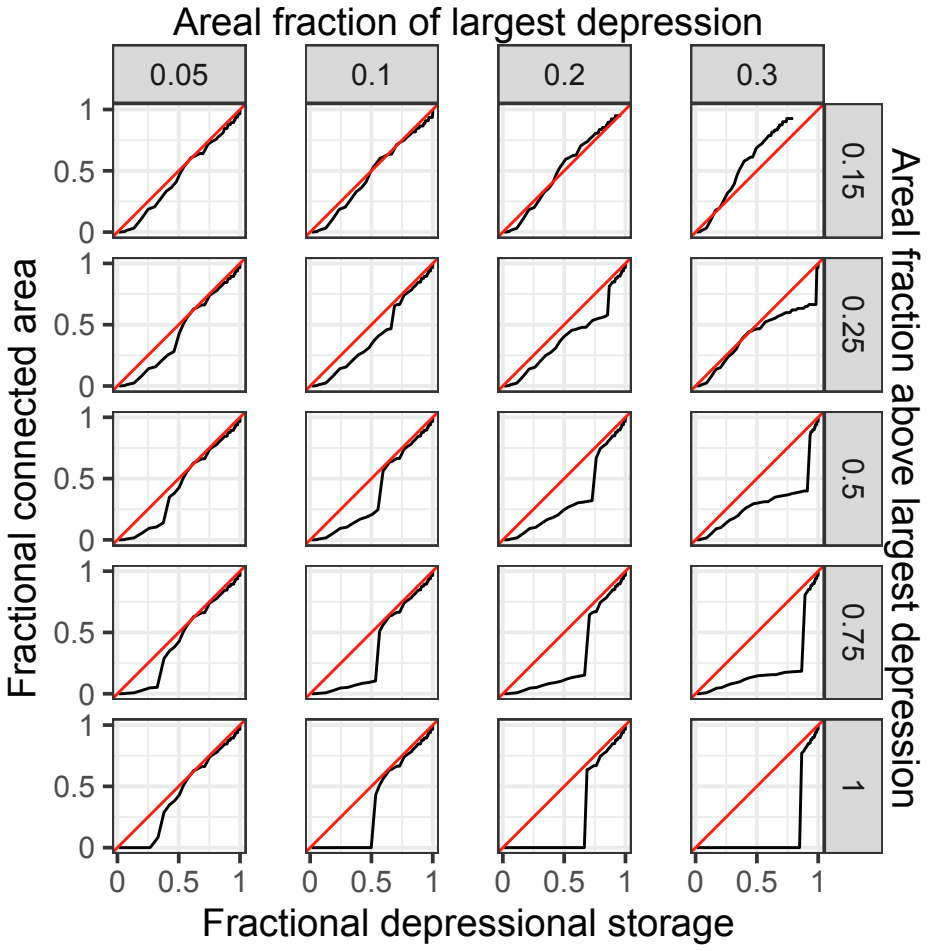


**Fig. 13.** The connected-fraction vs. the fractional storage for PCM models with varying locations and areal fractions of a single large pond. 1:1 lines are plotted in red.

Large basins, due to the simplifying effects of scale, may be amenable to representation by simplified models of their connected fractions, even when they contain a few very large depressions. In such a model the set of small depressions, which is hysteretic in its relationship between water storage and connected fraction, but does not show much gatekeeping, could be modelled as a single unit. The close alignment of the connected fraction curves with 1:1 lines on the rising limb indicate that it may be possible to approximate the hysteretic behaviour of the small depressions with linear relationship.

Where there are large depressions, i.e. with areas more than a few percent of the total, they would need to be simulated; this would not be the case in all basins. Large depressions are strong gatekeepers, but need not display hysteresis in their connected fractions if they are modelled individually. This would require determining the basin area, and the location in the overall basin, of each of the large depressions. The large depressions would receive runoff from the combined small depressions, in proportion to the large depressions' basin areas. When (if) the large depressions fill, they would permit flows to be contributed to the basin outlet. Such models would require only a few state variables, i.e. of the volume of water stored in the combined small depressions, and in each of the large depressions.

Although the two basins used as the bases for the analyses in this study, SDRB and SCRB, differ in many respects, they cannot represent all of the diversity of landscapes within the PPR. The development of a conceptual model separating gatekeeping and hysteresis and its incorporation within physically-based hydrological models would allow the conceptual model to be tested in other locations and would also allow the assessment of the effects of physical processes (and their spatio-temporal variabilities) on the variability of connected/contributing areal fractions of Prairie basins.

## CRediT authorship contribution statement

**Kevin Shook:** Conceptualization, Methodology, Formal analysis, Software, Data curation, Writing - original draft. **Simon Papalexiou:** Methodology, Formal analysis, Writing - original draft. **John W. Pomeroy:** Writing - original draft, Supervision, Funding acquisition.

## Declaration of Competing Interest

The authors declare that they have no known competing financial interests or personal relationships that could have appeared to influence the work reported in this paper.

## Acknowledgements

The authors acknowledge support from the Prairie Water Project of the CFREF Global Water Futures Programme, NSERC Changing Cold Regions Network, NSERC Discovery Grants, Canada Research Chairs and Canada Excellence Research Chairs programmes, Environment and Climate Change Canada, and Ducks Unlimited Canada.

## References

Ameli, A.A., Creed, I.F., 2019. Does wetland location matter when managing wetlands for watershed-scale flood and drought resilience? J. Am. Water Resour. Assoc. 55, 529–542. https://doi.org/10.1111/1752-1688.12737.

Armstrong, R., Kayter, C., Shook, K., Hill, H., 2013. Using the wetland dem ponding model as a diagnostic tool for prairie flood hazard assessment. In: Putting Prediction in Ungauged Basins into Practice. pp. 255–270.

Baker, N.T., 2011. National Stream Quality Accounting Network and National Monitoring Network Basin Boundary Geospatial Dataset, 200813 (USGS Numbered Series No. 641). U.S. Geological Survey, Reston, VA.

Bertassello, L.E., Rao, P.S.C., Jawitz, J.W., Botter, G., Le, P.V.V., Kumar, P., Aubeneau, A. F., 2018. Wetlandscape fractal topography. Geophys. Res. Lett. 45, 6983–6991. https://doi.org/10.1029/2018GL079094.

Bracken, L.J., Croke, J., 2007. The concept of hydrological connectivity and its contribution to understanding runoff-dominated geomorphic systems. Hydrol. Process. 21, 1749–1763. https://doi.org/10.1002/hyp.6313.

Bracken, L.J., Wainwright, J., Ali, G.A., Tetzlaff, D., Smith, M.W., Reaney, S.M., Roy, A. G., 2013. Concepts of hydrological connectivity: Research approaches, pathways and future agendas. Earth Sci. Rev. 119, 17–34. https://doi.org/10.1016/j.earscirev.2013.02.001.

Brannen, R., 2015. Controls on connectivity and streamflow generation in a Canadian Prairie landscape (MSc Thesis). University of Saskatchewan, Saskatoon, Saskatchewan, Canada.

Brannen, R., Spence, C., Ireson, A., 2015. Influence of shallow groundwater-surface water interactions on the hydrological connectivity and water budget of a wetland complex. Hydrol. Process. 29, 3862–3877. https://doi.org/10.1002/hyp.10563.

Brunet, N.N., Westbrook, C.J., 2012. Wetland drainage in the Canadian prairies: nutrient, salt and bacteria characteristics. Agric. Ecosyst. Environ. 146, 1–12. https://doi.org/10.1016/j.agee.2011.09.010.

Csardi, G., Nepusz, T., 2006. The igraph software package for complex network research. Int. J. Complex Syst. 1695, 1–9.

Dumanski, S., Pomeroy, J.W., Westbrook, C.J., 2015. Hydrological regime changes in a Canadian Prairie basin. Hydrol. Process. 29, 3893–3904. https://doi.org/10.1002/hyp.10567.

Evenson, G.R., Golden, H.E., Lane, C.R., D'Amico, E., 2015. Geographically isolated wetlands and watershed hydrology: a modified model analysis. J. Hydrol. 529, 240–256. https://doi.org/10.1016/j.jhydrol.2015.07.039.

Fang, X., Pomeroy, J.W., Westbrook, C.J., Guo, X., Minke, A.G., Brown, T., 2010. Prediction of snowmelt derived streamflow in a wetland dominated prairie basin. Hydrol. Earth Syst. Sci. 14, 991–1006. https://doi.org/10.5194/hess-14-991-2010.

Golden, H.E., Lane, C.R., Amatya, D.M., Bandilla, K.W., Raanan Kiperwas, H., Knightes, C.D., Ssegane, H., 2014. Hydrologic connectivity between geographically isolated wetlands and surface water systems: a review of select modeling methods. Environ. Model. Software 53, 190–206. https://doi.org/10.1016/j.envsoft.2013.12.004.

Government of Canada, 2013. ISO 19131 AAFC Watersheds Project – 2013 – Data Product Specification Revision: A. PFRA Sub-basins of the AAFC Watersheds Project – 2013.

Hayashi, M., Farrow, C.R., 2014. Watershed-scale response of groundwater recharge to inter-annual and inter-decadal variability in precipitation (Alberta, Canada). Hydrogeol. J. 22, 1825–1839. https://doi.org/10.1007/s10040-014-1176-3.

Hayashi, M., van der Kamp, G., 2000. Simple equations to represent the volume-area-depth relations of shallow wetlands in small topographic depressions. J. Hydrol. 237, 74–85. https://doi.org/10.1016/S0022-1694(00)00300-0.

Hayashi, M., van der Kamp, G., Rosenberry, D.O., 2016. Hydrology of Prairie wetlands: understanding the integrated surface-water and groundwater processes. Wetlands 36, 237–254. https://doi.org/10.1007/s13157-016-0797-9.

Hofert, M., Kojadinovic, I., Maechler, M., Yan, J., 2018. Copula: Multivariate dependence with copulas.

Hossain, K., 2017. Towards a Systems Modelling Approach for a Large-Scale Canadian Prairie Watershed (MSc Thesis). University of Saskatchewan, Saskatoon, Saskatchewan, Canada.

Kirkby, M.J., 1976. Tests of the random network model and its application to basin hydrology. Earth Surf. Processes 1, 197–212.

Kiss, J., 2018. Predictive mapping of wetland types and associated soils through digital elevation model analyses in the Canadian Prairie Pothole Region (Master's Thesis). University of Saskatchewan.

Leibowitz, S.G., Mushet, D.M., Newton, W.E., 2016. Intermittent surface water connectivity: fill and spill vs. fill and merge dynamics. Wetlands 36, 323–342. https://doi.org/10.1007/s13157-016-0830-z.

Liu, G., Schwartz, F.W., 2011. An integrated observational and model-based analysis of the hydrologic response of prairie pothole systems to variability in climate. Water Resour. Res. 47, 1–15. https://doi.org/10.1029/2010WR009084.

Mann, G.E., 1974. The prairie pothole region – a zone of environmental opportunity. Naturalist 25, 2.

McGuire, K.J., McDonnell, J.J., 2010. Hydrological connectivity of hillslopes and streams: characteristic time scales and nonlinearities. Water Resour. Res. 46 https://doi.org/10.1029/2010WR009341.

Mekonnen, M.A., Wheater, H.S., Ireson, A.M., Spence, C., Davison, B., Pietroniro, A., 2014. Towards an improved land surface scheme for prairie landscapes. J. Hydrol. 511, 105–116. https://doi.org/10.1016/j.jhydrol.2014.01.020.

Mengistu, S.G., Spence, C., 2016. Testing the ability of a semidistributed hydrological model to simulate contributing area. Water Resour. Res. 52, 4399–4415. https://doi.org/10.1002/2016WR018760.

Miller, J.J., Acton, D.F., St. Arnaud, R.J., 1985. The effect of groundwater on soil formation in a morainal landscape in Saskatchewan. Can. J. Soil Sci. 65, 293–307.

Minke, A.G., Westbrook, C.J., 2010. Water Storage of Prairie Potholes.https://doi.org/10.1007/s13157-010-0044-8.

Minke, A.G., Westbrook, C.J., van der Kamp, G., 2010. Simplified volume-area-depth method for estimating water storage of prairie potholes. Wetlands 30, 541–551. https://doi.org/10.1007/s13157-010-0044-8.

Mushet, D.M., Calhoun, A.J.K., Alexander, L.C., Cohen, M.J., DeKeyser, E.S., Fowler, L., Lane, C.R., Lang, M.W., Rains, M.C., Walls, S.C., 2015. Geographically isolated wetlands: rethinking a misnomer. Wetlands 35, 423–431. https://doi.org/10.1007/s13157-015-0631-9.

Nagler, T., Schepsmeier, U., Stoeber, J., Brechmann, E.C., Graeler, B., Erhardt, T., 2019. VineCopula: statistical inference of vine copulas.

Niazi, A., Bentley, L.R., Hayashi, M., 2017. Estimation of spatial distribution of groundwater recharge from stream baseflow and groundwater chloride. J. Hydrol. 546, 380–392. https://doi.org/10.1016/j.jhydrol.2017.01.032.

O'Kane, J.P., Flynn, D., 2007. Thresholds, switches and hysteresis in hydrology from the pedon to the catchment scale: a non-linear systems theory. Hydrol. Earth Syst. Sci. 11, 443–459. https://doi.org/10.5194/hess-11-443-2007.

Papalexiou, S.M., Serinaldi, F., 2020. Random fields simplified: preserving marginal distributions, correlations, and intermittency, with applications from rainfall to humidity. Water Resour. Res. 56 https://doi.org/10.1029/2019WR026331 e2019WR026331.

Papalexiou, S.M., Strnad, F., Markonis, Y., Shook, K., 2020. CoSMoS: Complete Stochastic Modelling Solution. R package version 2.0.0.

Phillips, R.W., Spence, C., Pomeroy, J.W., 2011. Connectivity and runoff dynamics in heterogeneous basins. Hydrol. Process. 25, 3061–3075. https://doi.org/10.1002/hyp.8123.

Pomeroy, J.W., Shook, K., Fang, X., Dumanski, S., Westbrook, C., Brown, T., 2014. Improving and Testing the Prairie Hydrological Model at Smith Creek Research Basin (No. 14). Centre for Hydrology, Saskatoon, Saskatchewan.

Rains, M., Leibowitz, S.G., Cohen, M.J., Creed, I.F., Golden, H.E., Jawitz, J.W., Kalla, P., Lane, C.R., Lang, M.W., McLaughlin, D.L., 2015. Geographically Isolated Wetlands are Part of the Hydrological Landscape. Hydrol. Process. 10.

R Core Team, 2013. R: A language and Environment for Statistical Computing. R Foundation for Statistical Computing, Vienna, Austria.

Schellenberg, G.J., 2017. Hydrology of the Delta Marsh Watershed: Water balance characterization and analysis of land use changes (MSc Thesis). University of Manitoba, Winnipeg, Manitoba, Canada.

Shapiro, M., Westervelt, J., 1992. R.MAPCALC. An Algebra for GIS and Image Processing. U.S. Army Construction Engineering Research Laboratory, Champaign, Illinois 61801, U.S.A.

Shaw, D.A., 2009. The influence of contributing area on the hydrology of the prairie pothole region of North America (PhD Thesis).

Shaw, D.A., Pietroniro, A., Martz, L.W., 2012a. Topographic analysis for the prairie pothole region of Western Canada. Hydrol. Process. 27, 3105–3114. https://doi.org/10.1002/hyp.9409.

Shaw, D.A., van der Kamp, G., Conly, F.M., Pietroniro, A., Martz, L., 2012b. The fill-spill hydrology of prairie wetland complexes during drought and deluge. Hydrol. Process. 26, 3147–3156. https://doi.org/10.1002/hyp.8390.

Shook, K., Pomeroy, J., van der Kamp, G., 2015. The transformation of frequency distributions of winter precipitation to spring streamflow probabilities in cold regions; case studies from the Canadian Prairies. J. Hydrol. 521, 395–409. https://doi.org/10.1016/j.jhydrol.2014.12.014.

Shook, K., Pomeroy, J.W., Spence, C., Boychuk, L., 2013. Storage dynamics simulations in prairie wetland hydrology models: evaluation and parameterization. Hydrol. Process. 27, 1875–1889. https://doi.org/10.1002/hyp.9867.

Shook, K.R., Pomeroy, J.W., 2011. Memory effects of depressional storage in Northern Prairie hydrology. Hydrol. Process. 25, 3890–3898. https://doi.org/10.1002/hyp.8381.

Spence, C., 2010. A paradigm shift in hydrology: storage thresholds across scales influence catchment runoff generation. Geogr. Compass 4, 819–833. https://doi.org/10.1111/j.1749-8198.2010.00341.x.

Stichling, W., Blackwell, S.R., 1957. Drainage area as a hydrologic factor on the glaciated canadian prairies. IUGG Proc. 111, 365–376.

Thapa, A., Bradford, L., Strickert, G., Yu, X., Johnston, A., Watson-Daniels, K., 2019. "Garbage in, Garbage Out" does not hold true for indigenous community flood extent modeling in the prairie pothole region. Water 11, 2486.

Tiner, R.W., 2003. Geographically isolated wetlands of the United States. Wetlands 23, 494–516. doi:10.1672/0277-5212(2003)023%5B0494:GIWOTU%5D2.0.CO;2.

van der Kamp, G., Hayashi, M., Bedard-Haughn, A., Pennock, D., 2016. Prairie pothole wetlands suggestions for practical and objective definitions and terminology. Wetlands 36, 229–235. https://doi.org/10.1007/s13157-016-0809-9.

Woo, M.-K., Rowsell, R.D., 1993. Hydrology of a prairie slough. J. Hydrol. 146, 175–207.

Zhang, B., Schwartz, F.W., Liu, G., 2009. Systematics in the size structure of prairie pothole lakes through drought and deluge. Water Resour. Res. 45 https://doi.org/10.1029/2008WR006878.